Optimized printing quality of battery electrode materials by laser-induced forward transfer

Ulrich Rist*
Institute for Applied Materials - Applied Materials Physics,
Karlsruhe Institute of Technology
Karlsruhe, Germany
https://orcid.org/0009-0006-3697-1687

Wilhelm Pfleging
Institute for Applied Materials - Applied Materials Physics,
Karlsruhe Institute of Technology
Karlsruhe, Germany
https://orcid.org/0000-0002-9221-9493

***Abstract*— With the ongoing global warming energy storages as lithium-ion batteries gain more importance due to the increasing amount of generated current with renewable energies. To further boost the battery development with the focus of advanced materials and architecture the LIFT-process offers a direct digital additive manufacturing tool for fast prototyping. In this work the impact of the printing quality in dependency of the particle size was investigated with the focus of the depiction of the laser beam profile with single voxels. Since electrode inks commonly consist of materials with different particle sizes the edge quality of printed areas was analyzed in dependency of the distance between the coated slurry and the substrate and the glycerol content in the solvent mixture. In the latter study, it was shown that a certain solvent mixture exhibits an optimized edge quality for a certain distance.**

Keywords — laser-induced forward transfer, nanoparticles, microparticles, anodes, lithium ion battery, printing quality

I. Introduction

With the ongoing global warming the urgent of CO_2-free energy generation technologies are becoming increasingly important. Renewable energies are often only generated temporarily (e.g. wind turbines and photovoltaics) and so the importance of energy storage is growing in order to ensure a continuous power supply. Lithium-ion batteries are so far one of the most promising electricity storage technologies for solving the challenges of energy storage. To further boost the energy density, power density and cyclability of lithium-ion cells high capacity materials as silicon are introduced to the batteries [1]. Additionally, optimized electrode architectures can boost the electrochemical properties of the electrodes. Structured electrodes provide additional space for the expansion of the materials during cycling, which is especially necessary with silicon, as it has a huge volume expansion of up to 300 % [2]. Also, multilayer electrodes can provide optimized electrochemical properties since the physical properties of the electrode, such as porosity or material composition, can be adjusted and the electrochemical properties of different used materials can be combined [3-5]. To further boost the development of optimized electrode architectures for lithium-ion batteries direct digital additive manufacturing processes can play an important role, by rapid prototyping [6]. Laser-induced forward transfer (LIFT) offers a versatile tool for printing electrodes, as changes to the geometry can be easily done by changing a CAD-file or the printing strategy. As LIFT is a nozzle-free printing process, the different particle sizes normally used in a battery slurry have no influence on the printability [7].

In research, nanoparticles [8-14] or even fluids [15-17] are often used in printing inks, but nano- to micro-sized particles are used in common battery production. In this work first, the influence of the particle size in the printing ink was investigated regarding how well the transferred voxel depict the laser profile geometry. Furthermore, for battery slurries with the same solid composition – materials with different particle sizes – but different solvent mixtures were analyzed in regard to the resulting edge quality at different process parameters.

II. Materials and Methods

The applied LIFT-process used in this work is displayed in Fig. 1. The LIFT-process for suspensions is according to the fluid transfer described by Fernádes-Pradas [18]. Material from the electrode ink getting partially evaporated. The resulting gas bubble expands and with the collapse of the bubble the material is transferred to the substrate which held in place by a vacuum chuck from below. The power source for the transfer is a tripled frequency Nd:YAG laser (Q301-HD-1000R, Lumentum, San Jose, CA, USA) with a resulting wavelength of 355 nm. The laser has a maximum power of 10 W, a pulse length of 78 ns and an optimized repetition rate of 10 kHz. Following the laser there is a diffractive optical element (DOE) with which the laser beam profile is transferred from a round gaussian one to a 175x175 µm^2 rectangle top-hat laser geometry. The rectangular laser geometry was used in the following to print the voxels and areas, but the laser beam geometry can be formed into squares or circles of different sizes by shadowing the remaining part of the laser beam with a subsequent mask selector. With an objective the laser is imaged with a demagnification factor of 3.5 on the backside of the electrode ink. The electrode ink was coated on a quartz glass wafer (DSP-200×0675-SGQ-00, Wafer Universe, Elsoff, Germany) via doctor blade with a coating gap of 40 µm. The glass wafer is referred as donor plate (DP) in the following.

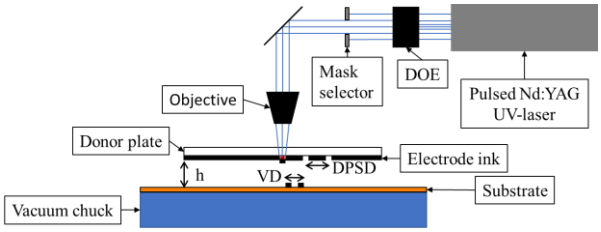

Fig. 1: Schematical illustration of the applied LIFT-process.

For the analyzation of the influence of the particle size on the printing quality different commonly used materials are used. As smallest particles carbon black (Super C65, C65, MTI Richmond, CA, USA) with an aggregate size of 100-500 nm [19] was under investigation, followed by conductive graphite (KS6L, Imerys, Paris, France) with a given diameter of d_{50} = 3.4 µm. As active materials flake-like graphite (T808, Targray, Kirkland, QC, Canada) with a given diameter of d_{50} = 7.5 µm was used in the analyzation. The materials were mixed with a binder solution with polyacrylic acid (PAA, 181285, Merck KGaA, Darmstadt, Germany) as binder and a mixture of deionized water and glycerol (99.6% purity, Thermo Scientific, Waltham, MA, USA) as solvent, with a ratio of water to glycerol of 1:1. The solid content was kept at 29.4 % except for the suspension with C65 there additional glycerol was added to decrease the solids content to 25 %, because of the resulting high viscosity with only sub-micrometer particles in the slurry. The ratio of the materials to PAA was set to 4:1. For the analyzation of the influence on the printing parameters and the amount of glycerol on the printing quality the battery slurry, a slurry with silicon (SI-15008, Kirkland, QC, Canada) and T808 graphite as active materials, PAA as binder and C65 as conductive additive were used. The composition of the solid materials can be found in TABLE I.

TABLE I: MATERIAL SOLID COMPOSITION OF THE USED BATTERY SLURRIES

Materials	**Composition in wt.%**
Silicon	40
PAA	20
T808	20
C65	20

All slurries were mixed with a planetary mixer (SpeedMixer DAC 150 SP, Hauschild, Hamm, Germany). For this purpose, the materials were mixed with the binder solution at speeds between 1000 rpm and 3500 rpm for at least 50 min until a homogeneous slurry was obtained.

After preparation, the slurries were coated on the DP via doctor blade with a coating gap of 40 µm. Before starting to print the coated donor plate was stored for 30 min under ambient conditions so a quasi- stationary state of the coating is realized. This is possible because glycerol has a low vapor pressure ($1.26 \times 10{-}5$ @ 20 °C [20]) and the most parts of water evaporates during the storage time.

For the analyzation of the printing quality of each voxel in dependency of the particle size the height h was adjusted between 100 µm to 500 µm. The laser fluence was varied between 0.14 J/cm^2 and 2.3 J/cm^2 within 48 steps. An example can be seen in Fig. 2a, at lower laser fluences no transfer occurred and so less than all 48 steps can be seen.

For the analyzation of the process parameters and the dependency of the solvent mixture to optimize the printing quality of a printed area different battery slurries according to the mixture displayed in TABLE I were manufactured. The glycerol content in the solvent was varied from 40 wt.% glycerol to 60 wt.% glycerol compared to water. For the laser parameter the distance between the coated slurry on the donor plate and the copper foil was adjusted from 150 µm to 750 µm. For each height first, a power variation was done to investigate the needed fluence for a transfer. Subsequently, the DPSD was adjusted, that the ablations on the DP are not affected by a previous ablation. Followed by a variation of the voxel distance to investigate at what distance a closed line can be still printed, according to [21]. The last variation was the variation of the printing speed, to see if there is a quality decrease with increasing the printing speed. With the analyzed parameters the area was printed at the end of the analyzation for each height. An exemplary illustration for the process is displayed in Fig. 2b.

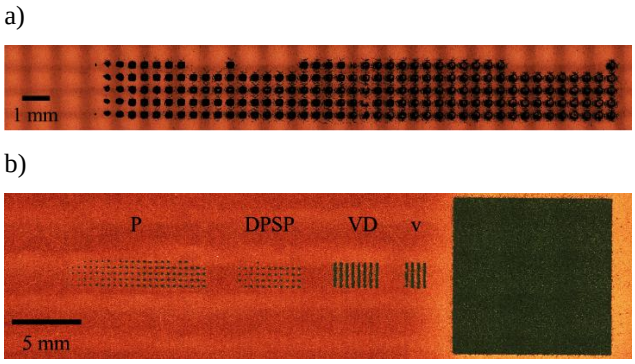

Fig. 2: Exemplary illustration of the respective experiments a) Variation of laser power to investigate the quality for different particle size (height: 150 µm, material: C65) and b) varitaion of process parameters for a solvent mixture (height: 550µm, glycerol content: 50 wt.%)

Subsequently to the printing, the geometries were dried for 24 h at a temperature of 80 °C, and a pressure of 10 mbar in a vacuum oven.

The printed geometries were analyzed visually via a digital microscope (VHX7000, Keyence Corporation, Ōsaka, Japan).

III. RESULTS AND DISCUSSION

In order to further improve the printing quality when printing with electrode ink, which commonly consists of different materials with different particle sizes, the influence of the particle size on the print quality was first investigated. In the first study the printing quality is referred to the imaging of the laser beam profile by a single voxel.

In Fig. 3a C65 with PAA was printed for this work the printing distance of 150 µm is exemplary analyzed. With the sub-micrometer particles, the transmitted voxel matches the laser beam profile well, but there is debris around the transmitted voxel. With increasing the particle size to d_{50} = 3.4 µm (KS6L) the laser profile geometry is not depicted as well as with the sub-micrometer particles, as can be seen in Fig. 3b. There are still transferred voxels that depict the laser profile geometry, but overall the type of geometry in the studied section appears quite random. With a further increase in particle size to a d_{50} = 7.5 µm (T808) – more than doubled to KS6L – there is no geometry of the transferred voxel recognizable anymore. However, further investigations are required to determine whether a comparable mass of material was nevertheless transferred. One assumption would be that the laser energy is mainly absorbed by the solid particles and that there are too many areas in the ink with the large particles where no solid particles are and therefore the laser can penetrate almost unhindered through the solvent, which means that there is significantly less energy available for a gas evolution and so for the transfer.

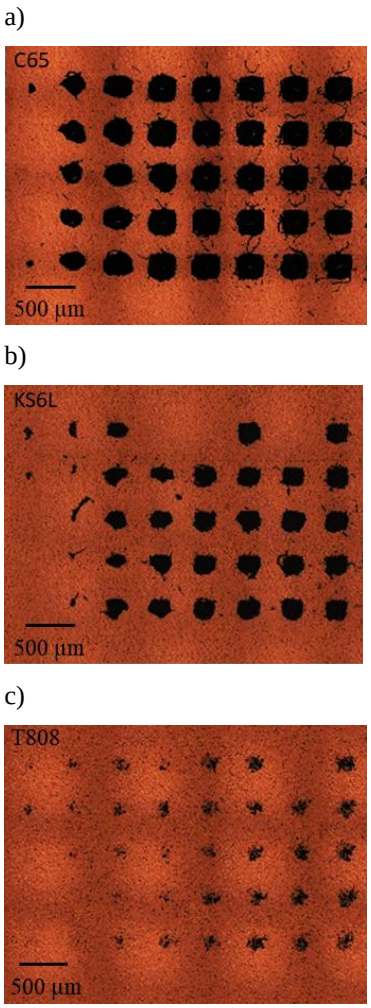

Fig. 3: Exemplary illustration of the examined print quality of different particle sizes at a transfer distance of 150 µm for the first 8 transferred voxels. For a) C65 (max. laser fluence: 0.70 J/cm^2), b) KS6L (max. laser fluence: 0.75 J/cm^2) and c) T808 (max. laser fluence: 1.54 J/cm^2)

In research it has been found that the viscosity of a nanoparticle paste plays an impact in the imaging of the laser beam profile by a transferred voxel [11]. The viscosities at a shear-rate of 50 1/s for the T808-, KS6L- and C65-slurries are 4.1 Pa·s, 18.6 Pa·s and 19.8 Pa·s, respectively. The C65 and KS6L slurries have a similar viscosity, so that the difference in the quality of the laser beam profile cannot be only explained by viscosity, but with the examined images also the particle size plays a role for the quality of a transferred voxel.

Since battery slurries are commonly manufactured with materials with different particle sizes the printing quality has to be optimized in a different way instead of the quality of a single transferred voxel. The ink composition for this section can be found in TABLE I. The following section examines how the edge quality of a printed area can be improved by changing two parameters: the distance between the coated slurry and the copper foil (h) and the glycerol content of the solvent. In Fig. 4 areas printed with optimized process parameters with two of the 5 used solvent mixtures are exemplary shown and will be discussed in the following. Fig. 4a reveals that the slurry manufactured with 60 wt.% glycerol, printed with a distance h of 150 µm pulled threads in the printing direction at the edge of the area during the printing process. This is also due to the consistence of the slurry due to the addition of glycerol. With increasing the distance between the coated slurry and the copper foil up to 550 µm (Fig. 4b) the slurry no longer pulls threads at the edge of the area. In research it has been shown that for low viscosities a liquid bridge was formed between the donor plate and the substrate during the transfer at a distance of 250 µm [12], and for larger distances more than 1 mm the material is transferred by a jet [11]. This indicates that the transfer mechanism changes and that either a liquid bridge no longer forms between the donor plate and the copper foil or the duration of the liquid bridge has been significantly reduced.

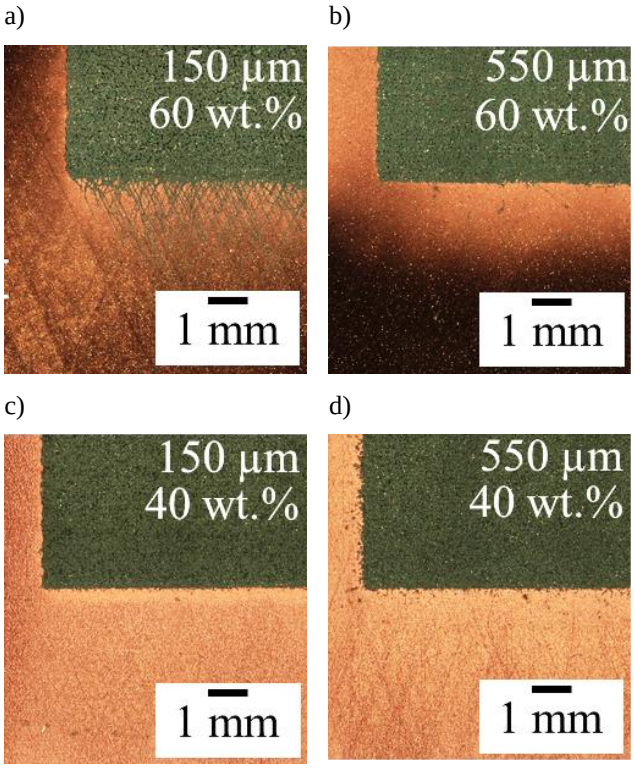

Fig. 4: Exemplary illustration of two solvent mixtures out of 5 examined ones, with a) h: 150 µm and glycerol content of 60 wt.%, b) h: 550 µm and glycerol content of 60 wt.%, c) h: 150 µm and glycerol content of 40 wt.%, d) h: 550 µm and glycerol content of 40 wt.%. The printing direction was in the vertical direction.

When reducing the glycerol content in the solvent down to 40 wt.% the slurry no longer pulls threads at the edge of the area at a distance h of 150 µm (Fig. 4c). The evaporation of the water prior to printing increases the viscosity, whereby the increase is higher with a lower glycerol content. This means that the viscosity of the slurry on the donor plate increases more in comparison to the slurry with 60 wt.% glycerol in the solvent due to the lower glycerol content, which could change the printing mechanism. With the increase of the distance h to 550 µm (Fig. 3d), the debris on the edge of the area increases and the edge becomes more irregular. For a slurry with 45 wt.% glycerol the optimized distance h is 350 µm, for the slurries with 50 wt.% glycerol and 55 wt.% glycerol it is between 350 µm and 550 µm because at 350 µm small threads are still occurring and at 550 µm the debris at the edges is increasing. Overall it can be stated, that if more glycerol is in the solvent the probability that the slurry pulls threads is increased at lower distances between the coated slurry and the copper foil. An increase in distance h or a decrease in the glycerol content helps to increase the edge quality of the printed area.

IV. Conclusion and Outlook

First the LIFT-process was performed using inks with only one kind of solid material and with PAA as binder. A power variation was performed at different heights to analyze the quality of the printing. For this analysis the printing quality was regarding to how well the transferred voxels depict the laser beam geometry. The submicrometer particles (C65) represent the laser beam profile best. Since the KS6L-ink has a similar viscosity, but represents less the laser beam profile the viscosity is not the only impact on the quality of the transfer, but also the particle size. The T808-ink shows no consistent voxel structure, further investigations are necessary for this slurry. Since the electrode ink commonly consists of different materials with different particle sizes an analyzation was performed with a silicon-containing electrode ink. Due to different particle sizes in the ink the edge quality of a printed area was the quality parameter instead of the quality of the single voxels. For the analyzation of the printing quality optimization of the process parameters and the glycerol content an area was printed after an optimization of the process parameter at different distances between the coated slurry on the donor plate and the copper foil. For different solvent mixtures different laser parameters are optimized. For example, for a glycerol content of 60 wt.% in the solvent a distance h of 550 µm showed a good edge quality, whereas for a glycerol content of 40 wt.% it needed only a distance h of 150 µm for a good edge quality. Therefore, a different distance between the slurry and the copper foil is optimal for each solvent mixture.

In further investigations the printings of the T808-ink hast to be analyzed, why the printed voxels have a random geometry. Furthermore, more materials should be used for the investigation of the printing quality of single voxels.

Acknowledgment

We are grateful to our colleague Marek Kapitz with the support in the laser processing and to the working group of Carsten Schroer for providing access to the Keyence VHX7000.

References

[1] W. Pfleging, P. Gotcu, P. Smyrek, Y. Zheng, J. K. Lee, and H. J. Seifert, "Lithium-Ion Battery—3D Micro-/Nano-Structuring, Modification and Characterization," vol. 309, pp. 313-347, 2020, doi: 10.1007/978-3-030-59313-1_11.

[2] L. Haneke *et al.*, "Insights into Electrolytic Pre-Lithiation: A Thorough Analysis Using Silicon Thin Film Anodes," (in eng), *Small*, vol. 19, no. 8, p. 2206092, Feb 2023, doi: 10.1002/smll.202206092.

[3] U. Rist, V. Falkowski, and W. Pfleging, "Electrochemical Properties of Laser-Printed Multilayer Anodes for Lithium-Ion Batteries," (in eng), *Nanomaterials (Basel)*, vol. 13, no. 17, pp. 1-20, Aug 25 2023, doi: 10.3390/nano13172411.

[4] L. Neidhart, K. Fröhlich, F. Winter, and M. Jahn, "Implementing Binder Gradients in Thick Water-Based NMC811 Cathodes via Multi-Layer Coating," *Batteries*, vol. 9, no. 3, p. 171, 2023, doi: 10.3390/batteries9030171.

[5] Y. Yuan, R. Hu, W. Wang, Y. Wang, T. Zhang, and Z. Wang, "Design and fabrication of high-performance multilayer silicon-carbon composite anodes for lithium-ion batteries via femtosecond laser," *J. Energy Storage*, vol. 110, 2025, doi: 10.1016/j.est.2025.115362.

[6] J. Holmström, M. Holweg, S. H. Khajavi, and J. Partanen, "The direct digital manufacturing (r)evolution: definition of a research agenda," *Oper. Manage. Res.*, vol. 9, no. 1-2, pp. 1-10, 2016, doi: 10.1007/s12063-016-0106-z.

[7] P. Serra and A. Piqué, "Introduction to Laser-Induced Transfer and Other Associated Processes," in *Laser Printing of Functional Materials. Electronics, 3D Microfabrication and Biomedicine*, A. Piqué and P. Serra Eds., 1. Auflage ed. Weinheim, Germany: Wiley-VCH Verlag GmbH & Co. KGaA, 2018, pp. 3-13.

[8] R. C. Auyeung, H. Kim, S. Mathews, and A. Pique, "Laser forward transfer using structured light," (in eng), *Opt Express*, vol. 23, no. 1, pp. 422-30, Jan 12 2015, doi: 10.1364/OE.23.000422.

[9] C. Boutopoulos, I. Kalpyris, E. Serpetzoglou, and I. Zergioti, "Laser-induced forward transfer of silver nanoparticle ink: time-resolved imaging of the jetting dynamics and correlation with the printing quality," (in English), *Microfluid. Nanofluid.*, vol. 16, no. 3, pp. 493-500, Mar 2014, doi: 10.1007/s10404-013-1248-z.

[10] [P. Delaporte and A. P. Alloncle, "[INVITED] Laser-induced forward transfer: A high resolution additive manufacturing technology," (in English), *Optics and Laser Technology*, vol. 78, pp. 33-41, Apr 2016, doi: 10.1016/j.optlastec.2015.09.022.

[11] S. A. Mathews, R. C. Y. Auyeung, H. Kim, N. A. Charipar, and A. Piqué, "High-speed video study of laser-induced forward transfer of silver nano-suspensions," (in English), *J. Appl. Phys.*, vol. 114, no. 6, p. 064910, Aug 14 2013, doi: 10.1063/1.4817494.

[12] P. Sopeña, J. M. Fernández-Pradas, and P. Serra, "Laser-induced forward transfer of low viscosity inks," *Appl. Surf. Sci.*, vol. 418, pp. 530-535, 2017, doi: 10.1016/j.apsusc.2016.11.179.

[13] F. Zacharatos, M. Makrygianni, and I. Zergioti, "Laser-Induced Forward Transfer (LIFT) Technique as an Alternative for Assembly and Packaging of Electronic Components," (in English), *IEEE J. Sel. Top. Quantum Electron.*, vol. 27, no. 6, pp. 1-8, Nov-Dec 2021, doi: 10.1109/Jstqe.2021.3084443.

[14] L. Rapp, J. Ailuno, A. P. Alloncle, and P. Delaporte, "Pulsed-laser printing of silver nanoparticles ink: control of morphological properties," (in eng), *Opt Express*, vol. 19, no. 22, pp. 21563-74, Oct 24 2011, doi: 10.1364/OE.19.021563.

[15] M. Colina, M. Duocastella, J. M. Fernández-Pradas, P. Serra, and J. L. Morenza, "Laser-induced forward transfer of liquids:: Study of the droplet ejection process," (in English), *J. Appl. Phys.*, vol. 99, no. 8, p. 084909, Apr 15 2006, doi: 10.1063/1.2191569.

[16] M. Duocastella, M. Colina, J. M. Fernández-Pradas, P. Serra, and J. L. Morenza, "Study of the laser-induced forward transfer of liquids for laser bioprinting," (in English), *Appl. Surf. Sci.*, vol. 253, no. 19, pp. 7855-7859, Jul 31 2007, doi: 10.1016/j.apsusc.2007.02.097.

[17] V. Dinca, M. Farsari, D. Kafetzopoulos, A. Popescu, M. Dinescu, and C. Fotakis, "Patterning parameters for biomolecules microarrays constructed with nanosecond and femtosecond UV lasers," (in English), *Thin Solid Films*, vol. 516, no. 18, pp. 6504-6511, Jul 31 2008, doi: 10.1016/j.tsf.2008.02.043.

[18] J. M. Fernández-Pradas, "Laser-Induced Forward Transfer of Fluids," in *Laser Printing of Functional Materials. Electronics, 3D Microfabrication and Biomedicine*, A. Piqué and P. Serra Eds., 1. Auflage ed. Weinheim, Germany: Wiley-VCH Verlag GmbH & Co. KGaA, 2018, pp. 63-89.

[19] H. Dreger, M. Huelsebrock, L. Froboese, and A. Kwade, "Method Development for Quality Control of Suspensions for Lithium-Ion Battery Electrodes," *Industrial & Engineering Chemistry Research*, vol. 56, no. 9, pp. 2466-2474, 2017, doi: 10.1021/acs.iecr.6b02103.

[20] P. Stephan *et al.*, Eds. *VDI-Wärmeatlas* (Springer Reference Technik). Berlin, Heidelberg: Springer Berlin Heidelberg, 2019, p. 2034.

[21] A. Palla-Papavlu, C. Córdoba, A. Patrascioiu, J. M. Fernández-Pradas, J. L. Morenza, and P. Serra, "Deposition and characterization of lines printed through laser-induced forward transfer," (in English), *Applied Physics a-Materials Science & Processing*, vol. 110, no. 4, pp. 751-755, Mar 2013, doi: 10.1007/s00339-012-7279-6.